Structure Preserving Stain Normalization of Histopathology Images Using Self Supervised Semantic Guidance

Dwarikanath Mahapatra[1(✉)], Behzad Bozorgtabar[2,3,4], Jean-Philippe Thiran[2,3,4], and Ling Shao[1,5]

[1] Inception Institute of Artificial Intelligence, Abu Dhabi, UAE
{dwarikanath.mahapatra,ling.shao}@inceptioniai.org
[2] Signal Processing Laboratory 5, EPFL, Lausanne, Switzerland
{behzad.bozorgtabar,jean-philippe.thiran}@epfl.ch
[3] Department of Radiology, Lausanne University Hospital, Lausanne, Switzerland
[4] Center of Biomedical Imaging, Lausanne, Switzerland
[5] Mohamed bin Zayed University of Artificial Intelligence, Abu Dhabi, UAE

Abstract. Although generative adversarial network (GAN) based style transfer is state of the art in histopathology color-stain normalization, they do not explicitly integrate structural information of tissues. We propose a self-supervised approach to incorporate semantic guidance into a GAN based stain normalization framework and preserve detailed structural information. Our method does not require manual segmentation maps which is a significant advantage over existing methods. We integrate semantic information at different layers between a pre-trained semantic network and the stain color normalization network. The proposed scheme outperforms other color normalization methods leading to better classification and segmentation performance.

Keywords: GANs · Semantic guidance · Color normalization · Digital pathology

1 Introduction

Increased digitization of pathology slides has enhanced the importance of digital histopathology in the medical imaging community. Staining is an important part of pathological tissue preparation where, e.g., Hematoxylin and Eosin dyes alter intensity of tissue elements - nuclei turns dark purple while other structures become pink. Tissue structures become distinguishable facilitating manual or automated analysis. Color variation of the same structure is observed due to differences in staining protocols from different centers, different dye manufacturers and scanner characteristics. Consequently, this leads to inconsistent diagnosis and limits the efficacy of automated methods. Hence there is a need for stain color normalization to have uniform appearance of dye-stained regions.

A. L. Martel et al. (Eds.): MICCAI 2020, LNCS 12265, pp. 309–319, 2020.
https://doi.org/10.1007/978-3-030-59722-1_30

We propose to integrate self-supervised semantic guidance with GANs for better structure preservation after stain normalization.

Two widely explored categories for stain normalization methods are color matching [23], and stain-separation [14,18]. Since these methods rely on template images it leads to mismatch and poor performance when the template is not representative of the dataset The third category comprises machine learning approaches [12] which sub-divide an input image into multiple tissue regions using a sparse autoencoder, and independently normalize each region. Recent works solve stain normalization as a style-transfer problem using Generative adversarial networks(GANs) [4]. GANs have found many applications in medical image analysis [13,32] such as image super-resolution [19], registration [22], segmentation [21,34] and augmentation [5,20] to name a few. Unpaired Image-to-Image Translation with CycleGANs were used in [26] to facilitate style transfer across two domains. These methods do not require a reference image and achieve high visual agreement with images from the target domain. Gupta et. al. in [10] leverage GAN based image-image translation for augmenting histopathology images to improve segmentation accuracy. Other variants include use of prior latent variables and auxiliary networks [33], and auxiliary inputs [35].

Previous works have demonstrated the effectiveness of cycle GANs in stain normalization, thus eliminating the tedious task of selecting a reference stain. However, as pointed out in [8] shape outlines of translated objects may change which leads to sub optimal performance. Gadermayr [8] used two different pipelines to overcome this pitfall. While their results are effective, the pipeline itself is tedious. Vahadane et al. [30] propose a structure preserving normalization method using non negative matrix factorization but do not explicitly use semantic information. Lahiani et al. [16] introduce a perceptual embedding loss to reducing tiling artifacts in reconstructed whole slide images (WSI).

Self-supervised learning requires formulating a proxy (or pretext) task which can be solved on the same dataset and using the trained network to perform self supervised tasks such as segmentation or depth estimation [9]. Some examples in the field of medical image analysis include surgical video re-colorization as a pretext task for surgical instrument segmentation [25], rotation prediction for lung lobe segmentation and nodule detection [29] and use disease bounding box localization for cardiac MR image segmentation [2].

Contributions: Since medical image analysis influences diagnostic decisions it is helpful to preserve information about finer structures for semantic guidance. Inclusion of segmentation information requires detailed annotations of the image which is extremely cumbersome for WSIs. Our primary contribution is a color stain normalization method that uses semantic guidance through self supervised features. We build our model using cyclic GANs [22,36] as they are an effective choice for transferring image appearances across domains. Semantic guidance is incorporated using a pre-trained semantic segmentation network trained on a different dataset. Semantic information in the form of segmentation feature maps from multiple levels is injected into the stain normalization network. Since

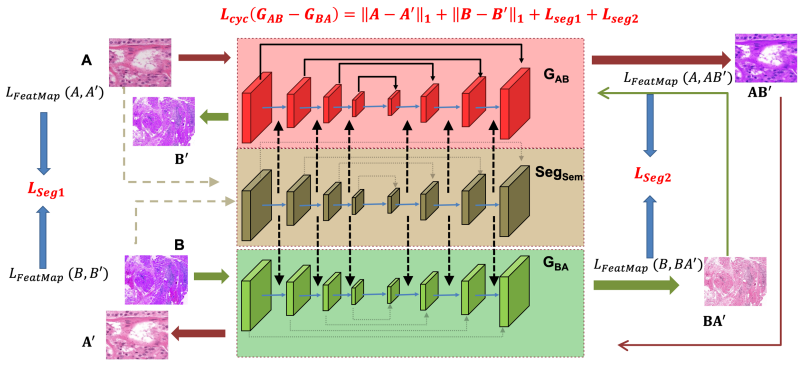

Fig. 1. Workflow of our proposed stain colour normalization method using CycleGANs. Semantic guidance is injected from the corresponding layers of Seg_{Sem} into the generators G_{AB}, G_{BA} and help preserve important cellular structures in normalization.

we use self supervised segmentation maps we do not need manual annotations during training or test stages which makes it easy to deploy for novel test cases.

Our paper makes the following contributions: 1) we integrate self-supervised features for stain normalization using semantic guidance from a pre-trained network; 2) self supervised segmentation feature maps allow us to use our method despite unavailability of manual segmentation maps. Our proposed method beats the state of the art stain normalization methods when the normalized images are used for classification and segmentation tasks. Different from [16], 1) we explicitly use semantic information to capture geometric and structural patterns for image normalization; 2) use pixel adaptive convolutions; and 3) match fine grained segmentation maps of normalized images.

2 Method

We denote the set of training images as I_{Tr}, their labels (manual segmentation masks or disease class) as L_{Tr}, and the trained model (segmentation or classification) as M_{Tr}. Given a set of test images I_{Test} our objective is to segment/classify them using the pre-trained model M_{Tr}. To successfully do that we : 1) color normalize the test images using our proposed method SegCN-Net; and 2) apply pre-trained M_{Tr}.

Figure 1 depicts the workflow of our proposed stain normalization method. There are three different networks, G_{AB} (the generator network in red), Seg_{Sem} (the pre-trained segmentation network in yellow providing semantic guidance), and G_{BA} (the generator network in green). All three networks are based on a UNet architecture [24] to facilitate easy integration of semantic information during training and test phases. G_{AB} transforms A to look like an image from domain B while G_{BA} performs the reverse translation to maintain cycle consistency. Images from A and B are passed through Seg_{Sem} and the information

from different layers of Seg_{Sem} is fused with the corresponding layer of G_{AB} and G_{BA} to facilitate integration of semantic guidance.

2.1 Semantic Guidance Through Self Supervised Learning

Our self-supervised approach does not define any pretext task but focuses on using pre-trained networks for semantic guidance in stain normalization. Semantic features for guiding the stain normalization task come from the pre-trained segmentation network Seg_{Sem} shown in Fig. 1. Seg_{Sem}'s pre-trained weights guide the feature learning process of the two generators without the need for further finetuning.

The translation invariance property of standard convolution makes it content-agnostic and poses certain limitations such as, despite reducing number of parameters it may lead to sub-optimal learning of feature representations. Additionally, spatially-shared filters globally average loss gradients over the entire image and the learned weights can only encode location-specific information within their limited receptive fields. Content-agnostic filters find it difficult to distinguish between visually similar pixels of different regions (e.g. dark areas due to artifacts or tissues) nor learn to identify similar objects of different appearance (e.g. same tissue structure with different shades as in our problem).

Pixel-adaptive convolutions [28] can address the above limitations where the feature representations encoded in the semantic network helps to distinguish between confounding regions, and are defined as

$$\mathbf{v}'_i = \sum_{j \in \Omega(i)} K(\mathbf{f}_i, \mathbf{f}_j) \mathbf{W} \left[\mathbf{p}_i - \mathbf{p}_j\right] \mathbf{v}_j + b \tag{1}$$

where $\mathbf{f}$ are the features from the semantic network that guide the pixel adaptive convolutions, $\mathbf{p}$ are pixel co-ordinates, $\mathbf{W}$ is the convolutional weights of kernel size k, Ω_i is a $k \times k$ convolution window around pixel i, $\mathbf{v}$ is the input and b is the bias term. For each feature map, we apply a 3×3 and a 1×1 convolution layer followed by Group Normalization [31] and exponential linear units (ELU) non-linearities [7]. The resulting semantic feature maps are fused with the corresponding layers of G_{AB} and G_{BA}, and used as guidance on their respective pixel-adaptive convolutional layers. K is a standard Gaussian kernel defined by

$$K(\mathbf{f}_i, \mathbf{f}_j) = \exp\left(-\frac{1}{2}(\mathbf{f}_i - \mathbf{f}_j)^T \Sigma_{ij}^{-1} (\mathbf{f}_i - \mathbf{f}_j)\right) \tag{2}$$

where Σ_{ij}^{-1} is the covariance matrix between feature vectors $\mathbf{f}_i$,$\mathbf{f}_j$ and formulated as a diagonal matrix $\sigma^2 \cdot I_D$, where σ is an additional learnable parameter for each filter. Standard convolution is a special case when $K(\mathbf{f}_i, \mathbf{f}_j) = 1$.

To capture semantic information across multiple scales we extract the feature maps after each convolution stage to get a set of maps with varying dimension due to max pooling operations, whose values are normalized to $[0, 1]$. For a given

pair of images we calculate the mean squared error between f_s - corresponding multi scale feature maps. Thus, the feature map loss between a and $\hat{a}$ is

$$L_{FeatMap}(a, \hat{a}) = \sum_{s=1}^{S} \sqrt{\frac{(f_s(a) - f_s(\hat{a}))^2}{N}} \tag{3}$$

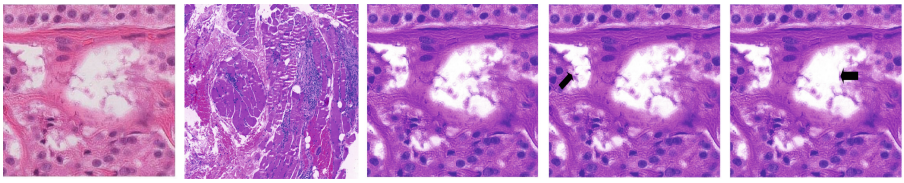

(a) (b) (c) (d) (e)

Fig. 2. Color normalization results: (a) Domain A image; (b) Domain B image; Domain A transformed to Domain B using: (c) proposed $SegCN - Net$; (d) [8]; (e) [35]. Areas of structure inconsistency are shown by black arrows. (Color figure online)

2.2 Color Normalization Using Semantic Guidance

Cycle GANs transform an image from domain A to B, and the reverse translation from B to A should generate the original input image. In forward cycle consistency, an image from domain A is translated to domain B by generator G_{AB} expressed as $a\hat{b} = G_{AB}(a)$. Image $a\hat{b}$ is translated back to domain A by G_{BA} to get $\hat{a} = G_{BA}(a\hat{b})$. Similarly, the original and reconstructed images from B should also match. Thus the overall cycle consistency loss is,

$$L_{cycle}(G_{AB}, G_{BA}) = E_a \left\| a - G_{BA}(G_{AB}(a)) \right\|_1 + \left\| b - G_{AB}(G_{BA}(b)) \right\|_1 + L_{Seg}, \tag{4}$$

$$L_{Seg} = \overbrace{L_{FeatMap}(a, \hat{a}) + L_{FeatMap}(b, \hat{b})}^{L_{Seg1}} + \overbrace{L_{FeatMap}(a, a\hat{b}) + L_{FeatMap}(b, b\hat{a})}^{L_{Seg2}} \tag{5}$$

We impose the additional constraint that the fine grained segmentation maps of images should match, not just of the reverse transformed images $a, \hat{a}$ and $b, \hat{b}$) but also between the outputs of each generator and the corresponding original images, i.e. between $a, a\hat{b}$ and $b\hat{a}, b$. L_{Seg2} is specifically designed to preserve structural information between images of domain A, B in stain normalization.

Discriminator D_B is employed to distinguish between real image b and generated image $a\hat{b}$ where the adversarial loss in forward cycle, L_{adv}, is

$$L_{adv}(G_{AB}, D_B, A, B) = E_b \log D_B(b) + E_a \log \left[(1 - D_B(G_{AB}(a))) \right]. \tag{6}$$

There also exists a corresponding $L_{adv}(G_{BA}, D_A, B, A)$ to distinguish between real image a and generated image $b\hat{a}$ Thus the final objective function is

$$L = L_{adv}(G_{AB}, D_B, A, B) + L_{adv}(G_{BA}, D_A, B, A) + L_{cyc}(G_{AB}, G_{BA}) \tag{7}$$

Network Architecture. All the networks ($G_{AB}, G_{BA}, Seg_{Sem}$) are based on a UNet architecture [24] with a ResNet backbone. Each convolution block has 3 layers of convolution layers (all using the pixel adaptive convolutions and ELU) followed by a 2×2 maxpooling step of stride 2. Skip connections exist between the stages of the contracting and expanding path. 3×3 kernels are used with adequate padding to maintain image dimensions. There are four convolution blocks in both paths.

3 Experimental Results

3.1 Evaluation Set up for Classification

Our proposed color normalization method is SegCN-Net (segmentation based color normalization network), and evaluate it's performance as a pre-processing step. CAMELYON16 [3] and CAMELYON17 [6] public datasets are used having WSIs for classification and segmentation of breast cancer metastases. CAMELYON16 has images from 2 independent medical centers while CAMELYON17's images come from 5 centers. We train SegCN-Net on CAMELYON16 and evaluate on transformed images of CAMELYON17. Domain A consists of images from Center 1 of CAMELYON16 ($C1_{16}$), while Domain B has images from $C2_{16}$. $100,000$ patches of 256×256 were extracted from each domain, and we train all models using a NVIDIA Titan X GPU having 12 GB RAM, Adam optimiser [15] with a learning rate of 0.002. Xavier initialization was used and training took 42 h for 150 epochs with batch size 16.

For evaluation, images from the different centers of CAMELYON17 were split into training/validation/test in 50/30/20% to obtain the following split: $C1_{17}$:37/22/15, $C2_{17}$: 34/20/14, $C3_{17}$: 43/24/18, $C4_{17}$: 35/20/15, $C5_{17}$: 36/20/15. For our first baseline, we train 5 different ResNet50 [11] with batch size 32, Adam optimizer learning rate of 0.001 for 70 epochs (denoted as $\mathbf{ResNet}_{NoNorm}$) on images from $C1_{17}$–$C5_{17}$ using the split described before, but without normalization. We apply SegCN-Net on images from different centers of CAMELYON17 to color normalize them and train ResNet50 networks with similar settings as $ResNet_{NoNorm}$ using the data split of $C1_{17}$–$C2_{17}$. The results (using area under curve (AUC) as the performance metric) are reported in Table 1 under SegCN-Net. We replace our stain normalization method with other competing methods, such as [8,18,23,30,35] and perform the same set of classification experiments with the performance summarized in Table 1.

[30] aims to preserve structure information through templates while [35] employ stain color matrix matching. Since they do not explicitly use segmentation information, SegCN-Net performs better than both methods. The method by [8] actually does better than others because of the use of segmentation information, but requires labeled segmentation maps. SegCN-Net's superior performance shows that use of self supervised segmentation can be leveraged when manual segmentation maps are not available. Figure 2 shows the stain normalized images of different methods. The advantage of SegCN-Net in preserving structural information is indicated by the black arrows where the glandular structure

is deformed from the original image in [35], and to a lesser extent in [8]. Thus the advantages of our semantic guidance based stain normalization is obvious.

Table 1. Classification results in terms of AUC measures for different stain normalization methods on the CAMELYON17 dataset. p values are with respect to SegCN-Net.

Method	Center 1	Center 2	Center 3	Center 4	Center 5	Average	p
$ResNet_{C17noNorm}$	0.8068	0.7203	0.7027	0.8289	0.8203	0.7758	0.0001
Reinhard [23]	0.7724	0.7934	0.8041	0.8013	0.7862	0.7915	0.0001
Macenko [18]	0.7148	0.7405	0.8331	0.7412	0.7436	0.7546	0.0001
CycleGAN	0.9010	0.7173	0.8914	0.8811	0.8102	0.8402	0.002
Vahadane [30]	0.9123	0.7347	0.9063	0.8949	0.8223	0.8541	0.003
Zhou [35]	0.9381	0.7614	0.7932	0.9013	0.9227	0.8633	0.013
Gadermayr [8]	0.9487	0.8115	0.8727	0.9235	0.9351	0.8983	0.013
SegCN-Net	**0.9668**	**0.8537**	**0.9385**	**0.9548**	**0.9462**	**0.9320**	-
Ablation Study Results							
SegCN-Net$_{Conv}$	0.9331	0.8255	0.9148	0.9259	0.9181	.9035	0.0008
SegCN-Net$_{Seg\ Only}$	0.9376	0.7974	0.8942	0.9187	0.9012	0.8898	0.0001
SegCN-Net$_{C17Rand}$	0.9624	0.8403	0.9267	0.9478	0.9391	0.9232	0.34
SegCN-Net$_{Glas}$	0.9762	0.8627	0.9509	0.9677	0.9588	0.9432	0.042

3.2 Ablation Studies

Table 1 summarizes the performance of the following variants of our method:

1. SegCN-Net$_{Conv}$ - $SegCN-Net$ using standard convolutions instead of pixel adaptive convolutions.
2. SegCN-Net$_{Seg}$ - SegCN-Net using only the final segmentation masks without the intermediate feature map. This evaluates the relevance of using a single segmentation map without semantic guidance at each layer.
3. SegCN-Net$_{C17Rand}$ - SegCN-Net tested on all normalized images of C17 with random selection of train/val/split. The results are an average of 10 runs and investigate possible bias in data split.

In the original approach Seg_{Sem} was pre-trained on the MS-COCO dataset [17]. In a variant of our proposed method we use a network pre-trained on the Glas segmentation challenge dataset [27] which has segmentation masks of histological images, and use it for classification of the test images from CAMELYON17. The results are shown in Table 1 under SegCN-Net$_{Glas}$.

SegCN-Net$_{Glas}$ shows better classification performance than SegCN-Net, and the difference in results at $p = 0.042$ is significant as semantic guidance is obtained from a network trained on histology images while SegCN-Net used

natural images. Although natural images provide some degree of semantic guidance by learning edge features, Seg_{Sem} trained on histopathology images provides domain specific guidance and hence leads to better performance. Since such a annotated dataset is not always available for medical images, we show that semantic guidance from a network trained on natural images significantly improves upon the state of art method for stain color normalization.

SegCN-Net$_{C17Rand}$ performance is close to SegCN-Net without any statistically significant difference, indicating that SegCN-Net is not biased on the test set. SegCN-Net$_{Seg\ Only}$ shows inferior performance compared to SegCN-Net, which indicates that multistage semantic guidance is much better than a single segmentation map. However SegCN-Net$_{Seg\ Only}$ still performs slightly better than [8] indicating the advantages of including segmentation information for structure preserving color normalization.

Table 2. Segmentation results on the GLas Segmentation challenge for $SegCN-Net$, [8,35] and the top ranked method. HD is in mm. Best results per metric in bold.

	$SegCN-Net$		Glas Rank 1		[8]		[35]	
	Part A	Part B	Part A	Part B	Part A	Part B	Part A	Part B
F1	**0.9351**	**0.7542**	0.912	0.716	0.926	0.728	0.922	0.729
DM	**0.9212**	**0.8054**	0.897	0.781	0.909	0.798	0.892	0.785
HD	**42.276**	**143.286**	45.418	160.347	44.243	157.643	47.012	161.321

3.3 Segmentation Results

We apply our method on the public GLAS segmentation challenge [27] which has manual segmentation maps of glands in 165 $H\&E$ stained images derived from 16 histological sections from different patients with stage $T3$ or $T4$ colorectal adenocarcinoma. We normalize the images using SegCN-Net (using MS-COCO images for semantic guidance), train a UNet with residual convolution blocks and apply on the test set. The performance metrics - Dice Metric (DM), Hausdorff distance (HD), F1 score (F1)- for SegCN-Net, [8,35] and the top ranked method [1] are summarized in Table 2. [35]'s performance comes close to the top ranked while [8] outperforms both of them, and SegCN-Net gives the best results across all three metrics. This shows that stain normalization in general does a good job of standardizing image appearance which in turn improves segmentation results. SegCN-Net performs best due to integration of segmentation information through self supervised semantic guidance.

3.4 Color Constancy Results:

Similar to [33] we report results for normalized median intensity, which measures color constancy of images, for the same dataset and obtained the following values:

SegCN-Net - Standard Deviation (SD) = 0.011, Coefficient of Variation (CV) = 0.021, which is better than Zanjani et al. [33] - $SD = 0.0188, CV = 0.0209$.

As reported in [16] we calculate values for complex wavelet structural similarity index (CWSSIM) between real and generated images. CWSSIM $\in [0, 1]$ with higher values indicating better match and is robust to small translations and rotations. Mean CWSSIM values of SegCN-Net is 0.82, which is higher than CycleGAN (0.75), [16] (0.77) and other baseline methods.

4 Conclusion

We have proposed a histopathology image stain color normalization approach using cycle GANs that integrates semantic guidance from self supervised segmentation feature maps. Our semantic guidance approach facilitates inclusion of segmentation information without the need for manually segmented maps that are very difficult to obtain. Experimental results on public datasets show our approach outperforms state of the art normalization methods when evaluated for classification and segmentation. Ablation studies also show the importance of semantic guidance. Although semantic guidance is obtained from the MS-COCO dataset of natural images, we also demonstrate that when domain specific guidance is used the results improve even further. This has potential in improving performance of medical image analysis tasks where annotations are not readily available.

References

1. Glas segmentation challenge results. https://warwick.ac.uk/fac/sci/dcs/research/tia/glascontest/results/. Accessed 30 Jan 2020
2. Bai, W., et al.: Self-supervised learning for Cardiac MR image segmentation by anatomical position prediction. In: Shen, D., et al. (eds.) MICCAI 2019. LNCS, vol. 11765, pp. 541–549. Springer, Cham (2019). https://doi.org/10.1007/978-3-030-32245-8_60
3. Bejnordi, B.E., Veta, M., van Diest, P.J., van Ginneken, B., Karssemeijer, N., Litjens, G., van der Laak, J.: Diagnostic assessment of deep learning algorithms for detection of lymph node metastases in women with breast cancer. JAMA **318**(22), 2199–2210 (2017)
4. BenTaieb, A., Hamarneh, G.: Adversarial stain transfer for histopathology image analysis. IEEE Trans. Med. Imaging **37**(3), 792–802 (2018)
5. Bozorgtabar, B., et al.: Informative sample generation using class aware generative adversarial networks for classification of chest Xrays. Comput. Vis. Image Underst. **184**, 57–65 (2019)
6. Bándi, P., et al.: From detection of individual metastases to classification of lymph node status at the patient level: The CAMELYON17 challenge. IEEE Trans. Med. Imaging **38**(2), 550–560 (2019)
7. Clevert, D.A., Unterthiner, T., Hochreiter, S.: Fast and accurate deep network learning by exponential linear units (ELUs). In: Proceedings of ICLR (2016)

8. Gadermayr, M., Appel, V., Klinkhammer, B.M., Boor, P., Merhof, D.: Which way round? a study on the performance of stain-translation for segmenting arbitrarily dyed histological images. In: Frangi, A.F., Schnabel, J.A., Davatzikos, C., Alberola-López, C., Fichtinger, G. (eds.) MICCAI 2018. LNCS, vol. 11071, pp. 165–173. Springer, Cham (2018). https://doi.org/10.1007/978-3-030-00934-2_19
9. Guizilini, V., Hou, R., Li, J., Ambrus, R., Gaidon, A.: Semantically-guided representation learning for self-supervised monocular depth. In: Proceedings of ICLR, pp. 1–14 (2020)
10. Gupta, L., Klinkhammer, B.M., Boor, P., Merhof, D., Gadermayr, M.: GAN-based image enrichment in digital pathology boosts segmentation accuracy. In: Shen, D., et al. (eds.) MICCAI 2019. LNCS, vol. 11764, pp. 631–639. Springer, Cham (2019). https://doi.org/10.1007/978-3-030-32239-7_70
11. He, K., Zhang, X., Ren, S., Sun, J.: Deep residual learning for image recognition. In: Proceedings of CVPR (2016)
12. Janowczyk, A., Basavanhally, A., Madabhushi, A.: Stain normalization using sparse autoencoders (STANOSA): application to digital pathology. Comput. Med. Imaging Graph **57**, 50–61 (2017)
13. Kazeminia, S., et al.: Gans for medical image analysis. In: arXiv preprint arXiv:1809.06222 (2018)
14. Khan, A., Rajpoot, N., Treanor, D., Magee, D.: A nonlinear mapping approach to stain normalization in digital histopathology images using image-specific color deconvolution. IEEE Trans. Biomed. Eng. **61**(6), 1729–1738 (2014)
15. Kingma, D.P., Ba, J.: Adam: a method for stochastic optimization. In: arXiv preprint arXiv:1412.6980 (2014)
16. Lahiani, A., Navab, N., Albarqouni, S., Klaiman, E.: Perceptual embedding consistency for seamless reconstruction of Tilewise style transfer. In: Shen, D., et al. (eds.) MICCAI 2019. LNCS, vol. 11764, pp. 568–576. Springer, Cham (2019). https://doi.org/10.1007/978-3-030-32239-7_63
17. Lin, T.-Y., et al.: Microsoft COCO: common objects in context. In: Fleet, D., Pajdla, T., Schiele, B., Tuytelaars, T. (eds.) ECCV 2014. LNCS, vol. 8693, pp. 740–755. Springer, Cham (2014). https://doi.org/10.1007/978-3-319-10602-1_48
18. Macenko, M., et al.: A method for normalizing histology slides for quantitative analysis. In: IEEE International Symposium on Proceedings of Biomedical Imaging: From Nano to Macro, ISBI 2009, pp. 1107–1110 (2009)
19. Mahapatra, D., Bozorgtabar, B., Hewavitharanage, S., Garnavi, R.: Image super resolution using generative adversarial networks and local saliency maps for retinal image analysis. In: Descoteaux, M., Maier-Hein, L., Franz, A., Jannin, P., Collins, D.L., Duchesne, S. (eds.) MICCAI 2017. LNCS, vol. 10435, pp. 382–390. Springer, Cham (2017). https://doi.org/10.1007/978-3-319-66179-7_44
20. Mahapatra, D., Bozorgtabar, B., Shao, L.: Pathological retinal region segmentation from oct images using geometric relation based augmentation. In: Proceedings of IEEE CVPR, pp. 9611–9620 (2020)
21. Mahapatra, D., Bozorgtabar, B., Thiran, J.-P., Reyes, M.: Efficient active learning for image classification and segmentation using a sample selection and conditional generative adversarial network. In: Frangi, A.F., Schnabel, J.A., Davatzikos, C., Alberola-López, C., Fichtinger, G. (eds.) MICCAI 2018. LNCS, vol. 11071, pp. 580–588. Springer, Cham (2018). https://doi.org/10.1007/978-3-030-00934-2_65
22. Mahapatra, D., Ge, Z.: Training data independent image registration using generative adversarial networks and domain adaptation. Pattern Recogn. **100**, 1–14 (2020)

23. Reinhard, E., Adhikhmin, M., Gooch, B., Shirley, P.: Color transfer between images. IEEE Comput. Graph. Appl. **21**(5), 34–41 (2001)
24. Ronneberger, O., Fischer, P., Brox, T.: U-Net: convolutional networks for biomedical image segmentation. In: Navab, N., Hornegger, J., Wells, W.M., Frangi, A.F. (eds.) MICCAI 2015. LNCS, vol. 9351, pp. 234–241. Springer, Cham (2015). https://doi.org/10.1007/978-3-319-24574-4_28
25. Ross, T., et al.: Gexploiting the potential of unlabeled endoscopic video data with self-supervised learning. Int. J. Comput. Assist. Radiol. Surg. **13**, 925–933 (2018)
26. Shaban, M.T., Baur, C., Navab, N., Albarqouni, S.: StainGAN: stain style transfer for digital histological images. arXiv preprint arXiv:1804.01601 (2018)
27. Sirinukunwattana, K., et al.: Gland segmentation in colon histology images: the GlaS challenge contest. Med. Imaging Anal. **35**, 489–502 (2017)
28. Su, H., Jampani, V., Sun, D., Gallo, O., Learned-Miller, E., Kautz, J.: Pixel-adaptive convolutional neural networks. In: Proceedings of IEEE CVPR, pp. 11166–11175 (2019)
29. Tajbakhsh, N., et al.: Surrogate supervision for medical image analysis: effective deep learning from limited quantities of labeled data. In: Proceedings of IEEE ISBI, pp. 1251–1255 (2019)
30. Vahadane, A., et al.: Structure-preserving color normalization and sparse stain separation for histological images. IEEE Trans. Med. Imaging **35**(8), 1962–1971 (2016)
31. Wu, Y., He, K.: Group normalization. In: Ferrari, V., Hebert, M., Sminchisescu, C., Weiss, Y. (eds.) ECCV 2018. LNCS, vol. 11217, pp. 3–19. Springer, Cham (2018). https://doi.org/10.1007/978-3-030-01261-8_1
32. Yi, X., Walia, E., Babyn, P.: Generative adversarial network in medical imaging: a review. Med. Imaging Anal. **58**, 101552 (2019)
33. Zanjani, F.G., Zinger, S., Bejnordi, B.E., van der Laak, J.A.: Histopathology stain-color normalization using deep generative models. In: Proceedings of Medical Imaging with Deep Learning (2018)
34. Zhao, M., et al.: Craniomaxillofacial Bony structures segmentation from MRI with deep-supervision adversarial learning. In: Frangi, A.F., Schnabel, J.A., Davatzikos, C., Alberola-López, C., Fichtinger, G. (eds.) MICCAI 2018. LNCS, vol. 11073, pp. 720–727. Springer, Cham (2018). https://doi.org/10.1007/978-3-030-00937-3_82
35. Zhou, N., Cai, D., Han, X., Yao, J.: Enhanced cycle-consistent generative adversarial network for color normalization of H&E stained images. In: Shen, D., et al. (eds.) MICCAI 2019. LNCS, vol. 11764, pp. 694–702. Springer, Cham (2019). https://doi.org/10.1007/978-3-030-32239-7_77
36. Zhu, J., Park, T., Isola, P., Efros, A.: Unpaired image-to-image translation using cycle-consistent adversarial networks. In: arXiv preprint arXiv:1703.10593 (2017)